ALTER: All-in-One Layer Pruning and Temporal Expert Routing for Efficient Diffusion Generation

Xiaomeng Yang[1*], **Lei Lu**[1*], **Qihui Fan**[1], **Changdi Yang**[1], **Juyi Lin**[1],
Yanzhi Wang[1], **Xuan Zhang**[1], **Shangqian Gao**[2†]
[1]Northeastern University [2]Florida State University
[1]{yang.xiaome, lu.lei1, fan.qih, yang.changd, lin.juy, yanz.wang,
xuan.zhang}@northeastern.edu [2]sgao@cs.fsu.edu

Abstract

Diffusion models have demonstrated exceptional capabilities in generating high-fidelity images. However, their iterative denoising process results in significant computational overhead during inference, limiting their practical deployment in resource-constrained environments. Existing acceleration methods often adopt uniform strategies that fail to capture the temporal variations during diffusion generation, while the commonly adopted sequential *pruning-then-fine-tuning strategy* suffers from sub-optimality due to the misalignment between pruning decisions made on pretrained weights and the model's final parameters. To address these limitations, we introduce **ALTER**: **A**ll-in-One **L**ayer Pruning and **T**emporal **E**xpoert **R**outing, a unified framework that transforms diffusion models into a mixture of efficient temporal experts. ALTER achieves a single-stage optimization that unifies layer pruning, expert routing, and model fine-tuning by employing a trainable hypernetwork, which dynamically generates layer pruning decisions and manages timestep routing to specialized, pruned expert sub-networks throughout the ongoing fine-tuning of the UNet. This unified co-optimization strategy enables significant efficiency gains while preserving high generative quality. Specifically, ALTER achieves same-level visual fidelity to the original 50-step Stable Diffusion v2.1 model while utilizing only 25.9% of its total MACs with just 20 inference steps and delivering a 3.64$\times$ speedup through 35% sparsity.

1 Introduction

Diffusion models [1, 2, 3] emerged as a leading class of generative models, achieving quality results in diverse tasks such as image generation [4, 5, 6, 7], image editing [8, 9] and personalized content generation [10, 11]. However, they face application limits due to costly inference: repeated full-network denoising causes latency and memory use, restricting real-time and low-resource deployment.

To mitigate the high computational cost of diffusion models, two primary strategies have emerged: one focuses on reducing the number of denoising steps in the temporal dimension, and the other explores model-level compression to reduce the per-step computational burden. Extensive research has been devoted to the former, including improved samplers [12, 13, 14], distillation methods [15] and feature caching [16]. In this work, we focus on the latter: *how model compression can be further improved to enhance efficiency without sacrificing performance?* Pruning has been a long-standing approach for reducing model complexity, with recent advances focusing on structured pruning to enable hardware-friendly acceleration. Among various structured pruning schemes, layer-wise

[*] Equal Contribution
[†] Corresponding Author

39th Conference on Neural Information Processing Systems (NeurIPS 2025).

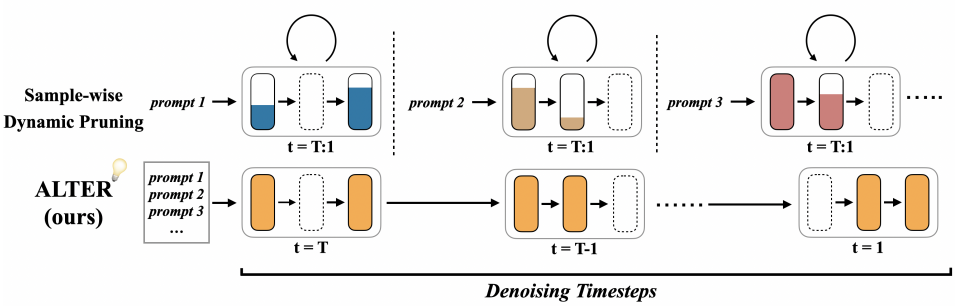

Figure 1: Comparison of model utilization in dynamic pruning. Sample-wise pruning can only use a static part of the model for one-specific image generation, while ALTER aims to achieve the full utilization of model capacity according to the necessity of each timestep.

pruning is the most practical in deployment, as it achieves speedup by discarding full layers with minimal modification to existing model execution pipelines. However, such coarse-grained pruning, especially when applied statically across all input prompts and denoising timesteps, often results in significant performance degradation due to both the complete removal of functional operators and the lack of flexibility to adapt to the varying computational demands.

To improve flexibility while retaining the deployment efficiency of layer-wise pruning, it is natural to combine dynamic pruning with coarse-grained structural removal, enabling different smaller models to be activated conditionally during inference. Existing efforts explore a sample-wise dynamic strategy, where a unique subnetwork is selected for each input [17, 18]. While this improves input adaptivity, it severely limits parameter utilization: *for a given sample, only a small subset of the model is used throughout the entire denoising trajectory.* To further unlock the potential of layer-wise pruning , we leverage the temporal asymmetry of diffusion, where different timesteps contribute unevenly to generation, to adaptively activate pruned substructures conditioned on the timestep, as shown in Fig. 1. This enables full model utilization across the trajectory, while suppressing redundant computation at each specific time step. While timestep-conditioned pruning improves overall parameter utilization, each substructure still requires fine-tuning to recover performance. Prior works often separate pruning and fine-tuning into distinct stages [19, 20], leading to a mismatch between fixed pruning decisions and evolving model weights. To address this, we propose to jointly optimize the pruning configuration and model parameters, allowing the substructures to co-adapt with the backbone during training.

To this end, we introduce the **A**ll-in-One **L**ayer **P**runing and **T**emporal **E**xpert **R**outing (ALTER) framework, a unified and one-stage optimization approach that seamlessly integrates layer pruning with temporal expert routing and model fine-tuning. It effectively transforms the standard diffusion model into a mixture of efficient temporal experts, where each expert is a specialized pruned subnetwork of the original model, tailored for distinct phases of the generation process. This dynamic configuration is achieved by identifying the optimal substructure for these different expert subnetworks and intelligently routing denoising timesteps to them throughout the entire finetuning phase. More specifically, we employ a hypernetwork to generate layer pruning decisions based on the updated model weights continuously, while managing the routing of timesteps to the appropriate experts at the same time. The impact of these pruning and routing decisions is simulated during training via a layer skipping mechanism in the forward pass. At inference time, the finalized hypernetwork allows for the selection of the most suitable expert and the skipping of designated layers for each timestep, thereby minimizing the temporal computational redundancy.

Our contributions can be summarized as follows:

(1) We propose ALTER: A novel framework that transforms diffusion models into a mixture of efficient temporal experts by unifying layer pruning, expert routing, and fine-tuning into a single-stage optimization process.

(2) Temporal Expert Routing: We introduce a hypernetwork-based mechanism that dynamically generates layer pruning decisions and manages timestep routing to specialized experts. Meanwhile, the shared denoising backbone is fully utilized by temporal experts to maximize parameter utilization.

(3) Strong Empirical Results: We conduct extensive experiments to show that ALTER significantly reduces computational costs (e.g., 25.9% FLOPs of 50-step Stable Diffusion v2.1) and accelerates inference (e.g., 3.64× speedup with 20 steps) thanks to the nature of layer-wise pruning while maintaining the same-level generative fidelity.

2 Related Work

2.1 Efficient Diffusion Models

Efforts to enhance the efficiency of diffusion models primarily explore two avenues: (1) sampling acceleration, such as fast samplers [21, 22, 13, 14, 12, 23, 24], step distillation [15, 25, 26, 27, 28, 29] and feature caching [16, 30, 31, 32, 33]. (2) model compression via techniques like pruning, quantization [34, 35], or efficient attention mechanisms [36]. And our work focus on pruning to compress the structure. Pruning aims to reduce model size and inference latency with minimal performance loss [37, 38, 39, 40, 41, 42, 43]. Unstructured pruning [44, 45, 46, 47] removes individual weights, leading to sparse patterns challenging to accelerate on common hardware. In contrast, structured pruning [48, 49, 50, 51, 52] removes entire components (e.g., channels, layers), yielding more readily deployable speedups. Within diffusion models, early structured pruning efforts often applied static pruning decisions [53]. For instance, LAPTOP-Diff [19] and LD-Pruner [20] identify and discard less important UNet layers, offering coarse-grained but highly efficient static pruning. However, the optimal model structure can vary significantly across the iterative denoising process. More recent advances have explored dynamic pruning [54], where the model learns to prune in a data- or context-dependent manner for flexibility in resource-constrained inference scenarios. APTP [18], for example, incorporates a prompt-routing model that learns and adaptively routes inputs to appropriate sub-architectures. However, although APTP's sample-wise approach improves adaptivity over static pruning, it typically commits to a single sub-model for the entire denoising trajectory, which can lead to under-utilization of the full model capacity. ALTER addresses this by introducing dynamism at the timestep level.

2.2 Mixture-of-Experts

Mixture-of-Experts (MoE) models [55, 56] conditionally activate only a subset of parameters during inference, offering a promising way to scale computation-expensive neural networks. While extensively utilized in large language models [57, 58], the application of MoE principles to enhance the efficiency of diffusion models remain less explored [59, 60]. APTP [18] highlights the potential of MoE interpretation in diffusion models by using a prompt router to convert each pruned model as an expert specializing in the assigned prompt. However, its reliance on routing each prompt to a fixed expert sub-model throughout the entire diffusion loop restricts model utilization and introduces parameter redundancy due to maintaining multiple expert copies. In light of this, we propose ALTER, where each expert is specialized for a specific range of timesteps and dynamically selected based on timestep embedding routing. Our method uniquely combines timestep-aware routing and structural pruning into a single-stage optimization framework for diffusion acceleration.

3 Method

ALTER restructures a standard diffusion UNet into a dynamic ensemble of temporal experts, each defined by a distinct layer-wise pruning configuration applied to the shared backbone. As shown in Fig. 2, a hypernetwork generates these binary pruning masks, and a lightweight router assigns each denoising timestep to an appropriate expert. All components are jointly optimized in a single-stage training process. During inference, the router dynamically activates expert-specific sub-networks conditioned on the timestep.

3.1 Preliminaries

Diffusion Process Diffusion models [2, 12] capture the data distribution by learning to reverse a predefined noising process applied to the input data. The forward process of the standard diffusion gradually adds Gaussian Noise to the clean input x_0 over T timesteps, generating a sequence of increasingly noisy latents $\{x_t\}_{t=1}^{T}$ with the assumption that x_T approximates pure noise. The reverse

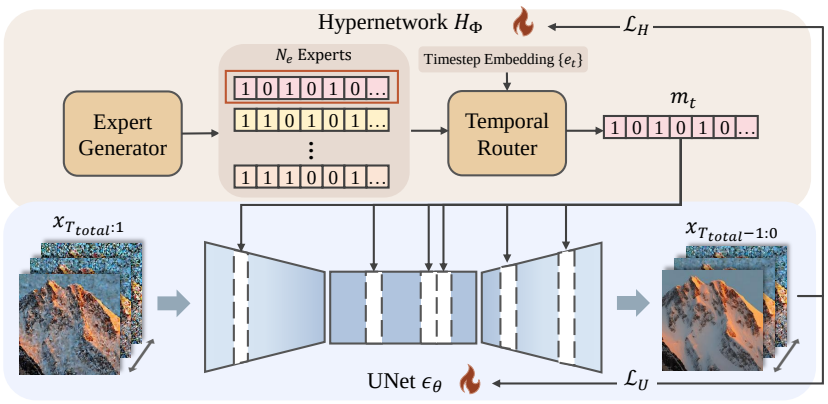

Figure 2: Overview of the ALTER framework. ALTER is a temporal-adaptive-pruning framework for diffusion models, where a hypernetwork generates layer-wise pruning configurations for expert subnetworks and assigns each denoising timestep to a corresponding expert.

process is modeled by a neural network $\epsilon_\theta(x_t, t, c)$ conditioned on the noisy sample x_t, the current timestep t, and optional context c (e.g., text embeddings). The network is trained denoise x_t into x_{t-1} by predicting the added noise at the t-th timestep, following the training objective:

$$\mathcal{L}_{\text{denoise}} = \mathbb{E}_{x_0,\epsilon\sim\mathcal{N}(0,I),t,c}\left[||\epsilon - \epsilon_\theta(x_t, t, c)||_2^2\right], \tag{1}$$

where $x_t = \sqrt{\bar{\alpha}_t x_0} + \sqrt{1-\bar{\alpha}_t}\epsilon$, and $\bar{\alpha}_t$ are predefined noise schedule coefficients. To enable the denoising network to adapt its behavior across different noise levels, the discrete timestep t is converted into a continuous vector embedding $e_t \in \mathbb{R}^{D_{emb}}$, where D_{emb} is the embedding dimension. This is often achieved using sinusoidal positional encodings [61] or learned embeddings. The timestep embedding e_t is then integrated into various layers of the neural network by adding it to the hidden activations within its blocks.

Layer-wise Pruning for Denoising Network. The denoising network ϵ_θ is commonly a UNet [62, 63], featuring an encoder-decoder structure with skip connections. Layer-wise pruning in the UNet architecture refers to the selective omission of entire pre-defined computational blocks, i.e, residual layers or transformer modules. To formalize the definition of pruning, we represent the configuration of a UNet with N_L prunable layers using a binary mask vector $m \in \{0,1\}^{N_L}$, where $m_i = 0$ indicates that the i-th layer is pruned, and $m_i = 1$ indicates that it is retained.

3.2 Temporal Expert Construction

ALTER employs a trainable hypernetwork $\boldsymbol{H}_\Phi$ to generate layer-wise pruning masks for a shared UNet backbone. These masks define N_e expert configurations, where each expert is equivalent to a layer-wise-pruned sub-network. $\boldsymbol{H}_\Phi$ consists of two trainable components whose trainable parameters jointly form Φ: (1) an Expert Generator $\boldsymbol{G}$ and (2) a Temporal Router $\boldsymbol{R}$.

Expert Generator. To generate N_e expert configurations, we employ Expert Generator $\boldsymbol{G}$ to produce a set of pruning masks $\{m_i\} \in [0,1]^{N_e \times N_L}$, where each $m_i \in [0,1]^{N_L}$ serves as the configuration for the i-th expert, $i \in \{1, \ldots, N_e\}$. The generator takes as input a set of frozen embeddings $Z \in \mathbb{R}^{N_e \times N_L \times D_{input}}$, initialized with orthogonal vectors, and processes them through several multi-layer perceptrons (MLPs) to produce a matrix of expert layer logits $L_{\text{experts}} \in \mathbb{R}^{N_e \times N_L}$. To approximate binomial distributions while retaining differentiability during training, we apply the Gumbel-Sigmoid function [64] combined with the Straight-Through Estimator (ST-GS) as the final layer on L_{experts} to obtain $\{m_i\}$.

Temporal Router. To select an appropriate expert for the t-th timestep in the diffusion process, we employ a Temporal Router $\boldsymbol{R}$ which shares a similar network structure with the expert configuration generator. The temporal router takes the corresponding pre-defined timestep embeddings $e_t \in \mathbb{R}^{D_{emb}}$ from the target UNet's timestep embedding mechanism as input, and maps it to the routing logits $L_t^{\text{routing}} \in \mathbb{R}^{N_e}$ over the N_e expert candidates. Similar to the expert configuration generator, we apply

the Gumbel-Softmax function with the Straight-Through Estimator to the routing logits to obtain the final categorical selection vector $\{s_t\}$.

By routing based on distinct timestep embeddings, the router enables expert specialization across different phases of the denoising trajectory, allowing the model to adaptively assign computation to the most suitable sub-network at each step.

Differentiable Simulation of Layer-wise Pruning. To simulate the effect of timestep-specific layer-wise pruning on the diffusion UNet during training, we modify the forward computation of each prunable layer $l \in \{1, \ldots, N_L\}$ as follows:

$$x_{\text{out}} = (1 - (m_t)_l) \cdot x_{\text{in}} + (m_t)_l \cdot f_l(x_{\text{in}}), \tag{2}$$

where x_{in} is the input to layer l, $f_l(\cdot)$ is the original layer computation, and $(m_t)_l \in [0, 1]$ denotes the pruning decision for layer l at timestep t. When $(m_t)_l = 0$, the layer is effectively skipped; when $(m_t)_l = 1$, it remains fully active. This formulation allows faithful simulation of pruning behavior while preserving gradient flow, enabling end-to-end optimization. The use of the Straight-Through Estimator (STE) in conjunction with Gumbel-Sigmoid and Gumbel-Softmax ensures differentiable sampling for both the pruning masks and the routing selection vector. During inference, we apply hard pruning by performing actual layer skipping whenever $(m_t)_l = 0$, thereby realizing computational efficiency through expert-specific subnetwork execution.

3.3 Optimization Strategy

ALTER, consisting of the shared UNet ϵ_θ with parameters θ and the hypernetwork $\boldsymbol{H}_\Phi$ with parameters Φ, is jointly optimized via a single-stage alternating training scheme. As detailed in Algorithm 1, each training step alternates between the following two optimization phases:

Shared UNet Backbone Optimization Given the N_e expert configurations $\mathcal{M}$ generated by the current hypernetwork $\boldsymbol{H}_\Phi$, the goal of shared UNet optimization is to ensure each expert substructure achieves strong denoising performance on its assigned group of timesteps. Thus, the primary training objective is the standard denoising loss $\mathcal{L}_{\text{denoise}}$, computed over masked subnetworks that simulate the active expert at each diffusion timestep. To further improve performance and stabilize training under layer-wise pruning, we optionally employ knowledge distillation from the frozen pretrained teacher model ϵ_T. Specifically, we introduce an output-level distillation loss $\mathcal{L}_{\text{outKD}}$, which encourages the student UNet $\epsilon_S \equiv \epsilon_\theta$ to produce similar denoising outputs as the teacher, and a feature-level distillation loss $\mathcal{L}_{\text{featKD}}$, which aligns intermediate representations between teacher and student. These auxiliary losses are defined as:

$$\mathcal{L}_{\text{outKD}} = \mathbb{E}[\|\epsilon_T(x_t, t, c) - \epsilon_S(x_t, t, c)\|_2^2], \ \mathcal{L}_{\text{featKD}} = \mathbb{E}[\Sigma_k \left\| f_T^k(x_t, t, c) - f_S^k(x_t, t, c) \right\|_2^2], \tag{3}$$

where f_T^k and f_S^k denote the k-th block feature activations from the teacher and student models, respectively. The total UNet loss combines the denoising objective and the distillation terms:

$$\mathcal{L}_U = \lambda_{\text{denoise}}\mathcal{L}_{\text{denoise}} + \lambda_{\text{outKD}}\mathcal{L}_{\text{outKD}} + \lambda_{\text{featKD}}\mathcal{L}_{\text{featKD}}, \tag{4}$$

where λ_{outKD} and λ_{featKD} are hyperparameters that control the influence of each distillation term.

Hypernetwork Optimization. Based on the current shared UNet backbone, the updated hypernetwork must satisfy three principles: (1) *Performance Preservation*: the temporal expert selected for a given denoising timestep should preserve the denoising capability depicted by the performance loss $\mathcal{L}_{\text{perf}}$ mirrors the UNet objective $\mathcal{L}_U$. It is evaluated using the masks m_t' from the trainable $\boldsymbol{H}_\Phi$ applied to the frozen UNet, ensuring $\boldsymbol{H}_\Phi$ generates effective masks maintaining good generation performance.

(2) *Structure Sparsity*: the temporal sparsity specialization throughout the diffusion trajectory should approach the user-defined computational reduction target. A sparsity regularization loss $\mathcal{L}_{\text{ratio}}(m_t')$ guides $\boldsymbol{H}_\Phi$ to achieve a target overall pruning ratio p. This term utilizes a log-ratio matching loss to penalize deviations of the current effective sparsity $S(m_t')$ from p. The precise method for calculating $S(m_t')$ based on layer costs and mask activations is detailed in Appendix B.2. $S(m_t')$ is a measure of the active portion of the network's FLOPs under mask m_t'. The loss is defined as:

$$\mathcal{L}_{\text{ratio}}(m_t') = \log\left(\frac{\max(S(m_t'), p)}{\min(S(m_t'), p) + \epsilon}\right), \tag{5}$$

Algorithm 1 ALTER Training Algorithm

Input: Training dataset $\mathcal{D}_{\text{train}}$; UNet ϵ_θ; Hypernetwork $\boldsymbol{H}_\Phi$; Total training steps T; Hypernetwork training end step T_{end}; Loss coefficients λ_{ratio}, λ_{balance}, λ_{outKD}, λ_{featKD}.
Initialization: Initialize UNet parameters θ; Initialize Hypernetwork parameters Φ (e.g., to output all-active masks).
$\mathcal{M} \leftarrow \boldsymbol{H}_\Phi(\text{eval=True})$ ▷ Initial mask configuration from $\boldsymbol{H}_\Phi$
for $t = 1$ **to** T **do**
  Sample a mini-batch s_b from $\mathcal{D}_{train}$;
  if $t \leq T_{\text{end}}$ **then** ▷ Hypernetwork Update
    $m'_t \leftarrow \boldsymbol{H}_\Phi(s_b, \text{train=True})$ ▷ Differentiable masks for batch s_b
    $\mathcal{L}_{\text{perf}} \leftarrow \mathcal{L}_{\text{denoise}}(\epsilon_\theta(s_b, \{m'_t\})) + \lambda_{\text{outKD}}\mathcal{L}_{\text{outKD}} + \lambda_{\text{featKD}}\mathcal{L}_{\text{featKD}}$ ▷ θ frozen
    Compute $\mathcal{L}_{\text{ratio}}(m'_t)$ and $\mathcal{L}_{\text{balance}}(m'_t)$;
    $\mathcal{L}_{\text{H}} \leftarrow \mathcal{L}_{\text{perf}} + \lambda_{\text{ratio}}\mathcal{L}_{\text{ratio}} + \lambda_{\text{balance}}\mathcal{L}_{\text{balance}}$;
    Update Φ with $\nabla_\Phi \mathcal{L}_{\text{H}}$;
    $\mathcal{M} \leftarrow \boldsymbol{H}_\Phi(\text{eval=True})$ ▷ Update mask from new $\boldsymbol{H}_\Phi$
  end if
  ▷ UNet Update
  Select masks $\{m_t\}$ for s_b from $\mathcal{M}$;
  $\mathcal{L}_{\text{UNet}} \leftarrow \mathcal{L}_{\text{denoise}}(\epsilon_\theta(s_b, \{m_t\})) + \lambda_{\text{outKD}}\mathcal{L}_{\text{outKD}} + \lambda_{\text{featKD}}\mathcal{L}_{\text{featKD}}$ ▷ Φ frozen
  Update θ with $\nabla_\theta \mathcal{L}_{\text{UNet}}$;
end for
Output: A fine-tuned UNet ϵ_θ and temporal mask decisions $\{m_t\}$.

where ϵ is a small constant for numerical stability.

(3) *Expert diversity*: The router should promote diverse expert selection across timesteps to prevent mode collapse. A router balance loss $\mathcal{L}_{\text{balance}}$ encourages diverse utilization of N_e experts [65, 66]:

$$\mathcal{L}_{\text{balance}} = N_e \sum_{i=1}^{N_e} F_i P_i, \tag{6}$$

where $F_i = \frac{1}{|\mathcal{B}|} \sum_{s_b \in \mathcal{B}} \mathbb{I}(\text{argmax}_j (L_{s_b}^{\text{routing}})_j = i)$ is the fraction of samples in batch $\mathcal{B}$ assigned to expert i, and $P_i = \frac{1}{|\mathcal{B}|} \sum_{s_b \in \mathcal{B}} (\text{Softmax}(L_{s_b}^{\text{routing}}))_i$ is the average router probability for expert i.

The total hypernetwork objective is

$$\mathcal{L}_H = \mathcal{L}_{\text{perf}} + \lambda_{\text{ratio}}\mathcal{L}_{\text{ratio}} + \lambda_{\text{balance}}\mathcal{L}_{\text{balance}}, \tag{7}$$

where λ_{ratio} and λ_{balance} are scalar coefficients. The differentiability of m'_t is achieved by ST-GS and ST-GSmax, whose implementation details are discussed in Appendix B.3. After updating the hypernet, the mask configuration $\mathcal{M}_U$ for subsequent UNet training steps is refreshed using the updated $\boldsymbol{H}_\Phi$. This alternating optimization strategy allows the UNet to adapt to the dynamic architectures from $\boldsymbol{H}_\Phi$, while $\boldsymbol{H}_\Phi$ learns to generate efficient and effective configurations. The hypernetwork would be trained until T_{end} is reached.

Such alternating training strategy enables the co-adaptation within ALTER: the UNet progressively recovers its denoising performance under various configurations of layer-wise sparsity, while the hypernetwork keeps refining the configurations and routing of specialized expert configurations tailored to the diffusion process.

4 Experiment

4.1 Experimental Setup

Implementation Details. We experiment on official pretrained diffusion model SDv2.1 [4] to demonstrate the effectiveness of our method. For training, we utilize a randomly sampled 0.3M subset of the LAION-Aestheics V2 (6.5+) [67]. We prune the models as 65% and 10 temporal experts with the loss weight $\lambda_{ratio} = 5$. The bi-level optimization takes 32k steps with global batch size 64, where the hypernetwork is trained for 2 epochs. All experiments are conducted on 2 A100 GPUs.

Table 1: Comparison with BK-SDM and APTP on CC3M and MS-COCO for SD-v2.1. The images are generated at the default resolution 768 and then downsampled to 256.

Method	Steps	CC3M					MS-COCO				
		MACs (G)(↓)	**Latency** (s)(↓)	**FID** (↓)	**CLIP** (↑)	**CMMD** (↓)	**MACs** (G)(↓)	**Latency** (s)(↓)	**FID** (↓)	**CLIP** (↑)	**CMMD** (↓)
SDv2.1 [4]	25	1384.2	4.0	17.08	30.96	0.361	1384.2	4.0	14.29	32.17	0.537
SDv2.1 [4]	20	1384.2	3.2	17.37	30.89	0.374	1384.2	3.2	14.46	32.08	0.532
BK-SDM-v2 (Base) [53]	25	876.5	2.5	17.53	29.77	0.486	876.5	2.5	19.06	30.67	0.654
BK-SDM-v2 (Small) [53]	25	863.2	2.5	18.78	29.89	0.453	863.2	2.5	20.58	30.75	0.645
APTP (0.85) [18]	25	1182.8	3.4	36.77	30.84	0.675	1076.6	3.1	22.60	31.32	0.569
APTP (0.66) [18]	25	916.3	2.6	60.04	28.64	1.094	890.0	2.5	39.12	29.98	0.867
ALTER (0.65) (Ours)	25	899.7	2.6	**16.74**	**30.94**	0.393	899.7	2.6	**13.70**	32.17	0.536
ALTER (0.65) (Ours)	20	899.7	2.1	17.14	30.92	**0.392**	899.7	2.1	13.89	**32.18**	**0.533**
ALTER (0.60) (Ours)	20	830.5	1.9	17.87	30.88	0.479	830.5	1.9	14.24	32.17	0.596

Datasets. We evaluate our proposed method on two widely-used diffusion benchmarks: Conceptual Captions 3M [68] (CC3M) and MS-COCO [69]. We evaluate pruning methods using 14k samples in the validation set of CC3M and 30k samples from the MS-COCO 2014's validation split. We sample the images at the default 768 resolution and then resize them to 256 for calculating the metrics with the PNDM [22] sampler following previous works [53, 18]. To compare with previous cache method, we also experiment on the COCO 2017's 5k validation dataset.

Evaluation Metrics. We report FID (↓) [70] and CMMD (↓) [71] to assess image quality, CLIP (↑) score [72] to measure text–image alignment, the number of multiply–accumulate operations (MACs) (↓) as a proxy for computational cost, and wall-clock inference latency in seconds (Latency) (↓). We also report the speedup of ALTER compared with the original model. The MACs and latency are measured with batch size 1 in the A100 GPU platform.

4.2 Comparison Results

Comparison with Static and Sample-wise Dynamic Pruning Method. We benchmark ALTER against two representative pruning baselines: BK-SDM-v2 [53], which employs static pruning, and APTP [18], which utilizes a sample-wise Mixture-of-Experts (MoE) approach conditioned on input prompts. As detailed in Table 1, ALTER consistently demonstrates superior generative quality and competitive efficiency. Specifically, during a 25-step inference on MS-COCO, ALTER achieves a leading FID of 13.70 and a CLIP score of 32.17, which outperforms BK-SDM-v2 (Small) and APTP (0.66), while operating at comparable computational costs. Similar advantages for ALTER are observed on the CC3M dataset. Remarkably, ALTER's efficiency allows for even stronger performance with fewer steps. With only 20 inference steps, ALTER still surpasses the 25-step performance of both BK-SDM-v2 and APTP, highlighting its superior trade-off between speed and quality. Furthermore, ALTER's performance at both 25 and even 20 steps is not only competitive with but even exceeds that of the original unpruned SDv2.1 model. These comprehensive results confirm that ALTER's strategy of routing masks by timestep, rather than relying on a single global pruning or solely on prompt-based cues, allocates model capacity more precisely to the varying demands of the diffusion process. Qualitative comparisons presented in Figure 3 visually affirm these findings, showcasing that images generated by ALTER exhibit a quality comparable to the unpruned SD-v2.1 model and display fewer artifacts than those produced by BK-SDM-v2.

Comparison with Cache-Based Method. We further evaluate ALTER against DiP-GO [30], a leading cache-based acceleration technique, on the MS-COCO 2017 validation set, with results detailed in Table 2. Cache-based methods primarily aim to reduce computation by reusing features from previous timesteps. While effective, they often operate on the original model architecture and may require careful tuning of parameters like cache rate [16] for optimal performance with different inference schedules. In contrast, ALTER's temporal pruning-based approach results in an inference schedule-agnostic model. Once the hypernetwork has determined the temporal expert structures and routing, the resulting dynamically pruned UNet can be deployed with any number of denoising steps without retraining or specific adjustments, offering significant operational flexibility.

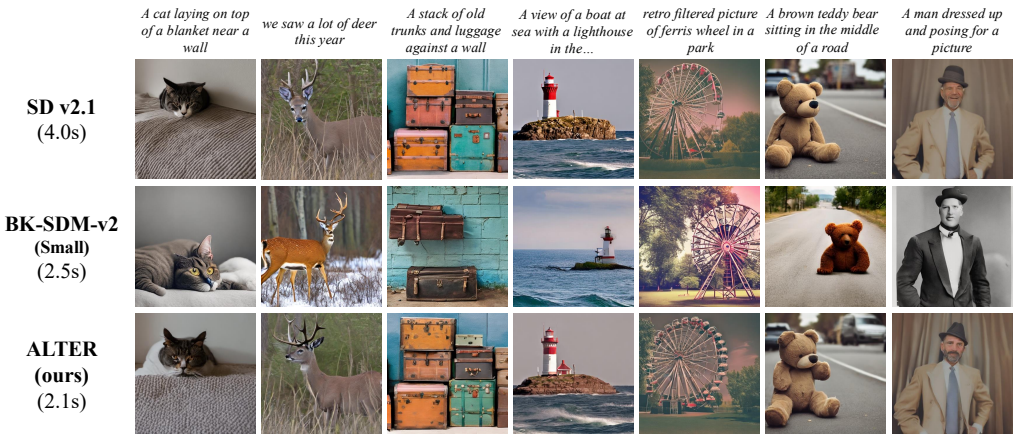

Figure 3: A qualitative comparison with original SDv2.1 and BK-SDM-Small. SDv2.1 and BK-SDM-Small adopt the 25-step PNDM while our method adopts the 20-step inference.

Table 2: Comparison with DiP-GO on the MS-COCO 2017 validation set on SD-2.1. MACs here is the total MACs for all steps.

Method	**MACs**(↓)	**Speedup**(↑)	**CLIP** (↑)	**FID-5K** (↓)
SDv2.1 (50 steps) [4]	38.04T	1.00×	31.55	27.29
SDv2.1 (20 steps) [4]	15.21T	2.49×	31.53	27.83
DiP-GO (0.7) [30]	11.42T	3.02×	31.50	25.98
ALTER (0.65) (Ours) (20steps)	9.89T	3.64×	**31.62**	**25.25**
SDv2.1 (15 steps)	11.41T	3.23×	30.99	27.46
DiP-GO (0.8) [30]	7.61T	3.81×	30.92	27.69
ALTER (0.65) (Ours) (15steps)	7.42T	4.37×	**31.19**	**26.58**

For a 20-step inference process, ALTER significantly reduces total MACs to 9.89T, which is a substantial improvement over the original SDv2.1 and achieves a 3.64× speedup compared to the 50-step SDv2.1 baseline, while delivering generative quality that is comparable or even superior (e.g., FID-5K of 25.25 for ALTER vs. 27.83 for SDv2.1 20-steps and 27.29 for SDv2.1 50-steps). ALTER (20 steps) is also more computationally efficient than DiP-GO (0.7) and demonstrates superior performance scores. When the inference step is further reduced to 15 steps, ALTER maintains strong generative quality and achieves better performance compared with the 15-step SDv2.1. It again outperforms DiP-GO (0.8) in both efficiency and generative quality. This robust ability to adapt to various inference steps without re-tuning demonstrates ALTER's suitability for real-time applications.

4.3 Abalation Study

Ablation Study on ALTER's Key Components. To evaluate the contributions of ALTER's key design components, the usage of multiple specialized experts, the temporal router and the single-stage joint optimization strategy, we conduct a comprehensive ablation study. As shown in Table 3, we compare the full ALTER framework against three variants: (1) "Static", which employs a static global pruning pattern across all timesteps; (2) "Manual", which introduces multiple experts but assigns them to predefined fixed timestep intervals instead of employing a learnable router; (3) "TwoStage", which incorporates ALTER's architecture but adopts a two-stage optimization approach where the hypernetwork is trained first, followed by fine-tuning the UNet.

The results clearly demonstrate the benefits of each component. The "Static" variant, lacking specialized temporal handling, expectedly exhibits the worst performance. Transitioning to the "Manual" approach, which introduces multiple experts for different fixed temporal intervals, yields a significant improvement (e.g., FID drops from 19.03 to 17.91 on CC3M). This demonstrates the importance of having specialized experts for different phases of the denoising process. Further introducing the learnable timestep router in ALTER provides an additional performance boost over

Table 3: Ablation study on pruning and optimization strategies.

Variant	Multi Expert	Timestep Router	Joint Training	CC3M			MS-COCO		
				FID (↓)	CLIP (↑)	CMMD (↓)	FID (↓)	CLIP (↑)	CMMD (↓)
Static	✗	✗	✓	19.03	30.75	0.397	15.35	32.01	0.544
Manual	✓	✗	✓	17.91	30.82	0.427	14.13	32.08	0.571
TwoStage	✓	✓	✗	17.65	30.88	0.401	14.45	32.02	0.539
ALTER	✓	✓	✓	**17.14**	**30.92**	**0.392**	**13.89**	**32.18**	**0.533**

Table 4: Comparison with TinyFusion and DyDiT for DiT-XL/2 on ImageNet of 256×256 resolution.

Method	Speedup	IS(↑)	FID(↓)	sFID(↓)	Precision(↑)	Recall(↑)
DiT-XL/2 [7] (28-layer)	1.00×	277.00	2.27	4.60	0.83	0.57
DyDiT-XL [54] (λ=0.5)	1.72×	248.03	2.07	4.56	0.80	0.61
TinyFusion [73] (14-layer)	1.96×	234.50	2.86	4.75	0.82	0.55
ALTER (Ours) (avg. 14-layer)	1.92×	254.29	2.36	4.63	0.82	0.58

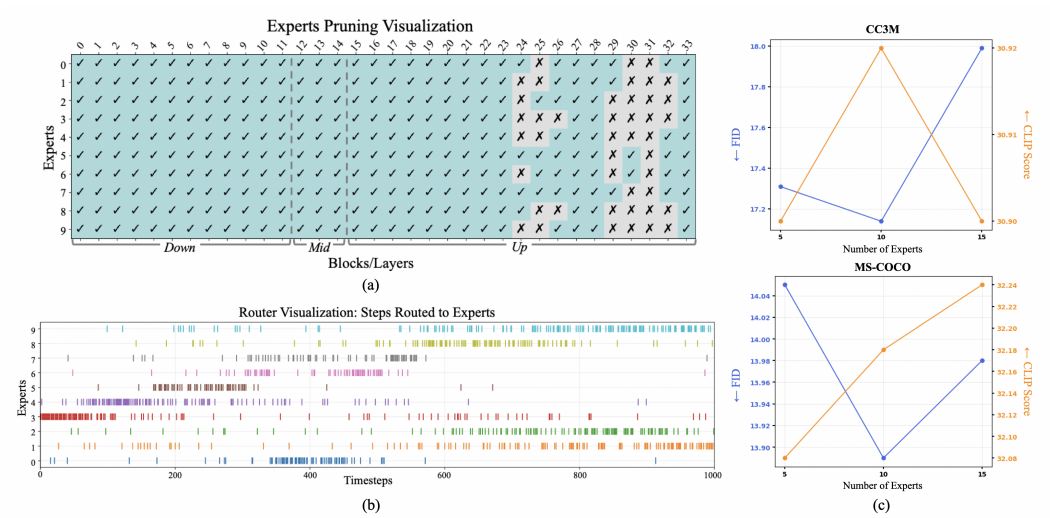

Figure 4: ALTER (0.65)'s temporal experts and router behavior. (a) Visualization of pruning patterns for $N_e = 10$ experts. (b) Visualization of timestep-to-expert routing dynamics. (c) Ablation results for the number of experts on CC3M and MS-COCO 2014.

the "Manual" variant's coarse-grained, fixed assignments, reducing FID to 17.14 on CC3M and 13.89 on MS-COCO, which underscores the benefits of a dynamically learned, fine-grained temporal routing mechanism. Finally, the comparison between ALTER and the "TwoStage" optimization variant shows the critical advantage of our single-stage joint optimization strategy, which facilitates the co-adaptation of UNet's generative ability with the hypernetwork, leading to superior generative quality across all evaluated metrics on both datasets. These ablation experiments collectively validate the effectiveness and contributions of ALTER's key design choices.

Analysis of Temporal Experts To understand the characteristics of the temporal experts learned by ALTER, we analyze their pruning patterns, routing dynamics, and the impact of number of experts, as shown in Figure 4. The visualization of pruning patterns for the $N_e = 10$ experts (Fig 4(a)) demonstrates structural diversity. Different experts adopt distinct pruning patterns across the UNet blocks and layers. For instance, some experts being heavily pruned (e.g., experts 3,8,9) while some retain greater capacity (e.g., experts 5-7). This learned structural differentiation allows for temporal specialization. The router dynamics in Fig. 4(b) illustrates how these specialized experts are allocated across different denoising timesteps. We observe that specific experts are predominantly active during certain phases of the diffusion process. Furthermore, the ablation study on the number of experts highlights the importance of an adequate expert number for achieving optimal performance,

as shown in Fig. 4(c). Our chosen configuration of $N_e = 10$ experts consistently yields the best or near-best FID and CLIP scores on both CC3M and MS-COCO datasets. Performance tends to degrade with fewer experts, likely due to insufficient capacity for fine-grained temporal specialization across the entire denoising process. Conversely, increasing to $N_e = 15$ experts does not yield further improvements and can sometimes slightly degrade performance, potentially due to challenges in effectively training a larger set of specialized experts or increased complexity in the routing decisions.

Generality to DiT. To assess generality beyond U-Nets, we apply *ALTER* to a DiT-XL/2 backbone [7] and evaluate on ImageNet [74] at 256×256 using a 250-step DDPM sampler [2]. As shown in Table 4, our method achieves a $1.92\times$ speedup while maintaining an FID score (2.36) comparable to the full model (2.27). With approximately half the layers active on average, our method significantly outperforms static pruning (TinyFusion [73]), especially on key quality metrics like IS (254.29 vs. 234.50) and FID (2.36 vs. 2.86). When comparing to dynamic methods like DyDiT [54], ALTER brings higher speedup. It is important to note that our approaches are orthogonal and complementary. ALTER performs coarse-grained layer-level pruning, while DyDiT performs fine-grained pruning within each block. This empirically confirms that our framework is effective beyond U-Nets and is applicable to modern Transformer-based architectures.

5 Conclusion

In this paper, we presented an acceleration framework ALTER that transforms the diffusion model to a mixture of efficient temporal experts by employing a trainable hypernetwork to dynamically generate layer pruning decisions and manage timestep routing to specialized, pruned expert subnetworks throughout the ongoing fine-tuning of the UNet. This timestep-wise approach overcomes the limitations of static pruning and sample-wise dynamic methods, enabling superior model capacity utilization and denoising efficiency. The experiments under various settings and ablation analysis demonstrate the effectiveness of ALTER, which could achieve a 3.64× speedup on the original SDv2.1 with 35% sparsity.

References

[1] Yang Song and Stefano Ermon. Generative modeling by estimating gradients of the data distribution. *Advances in neural information processing systems*, 32, 2019.

[2] Jonathan Ho, Ajay Jain, and Pieter Abbeel. Denoising diffusion probabilistic models. *Advances in neural information processing systems*, 33:6840–6851, 2020.

[3] Sungbin Lim, Eunbi Yoon, Taehyun Byun, Taewon Kang, Seungwoo Kim, Kyungjae Lee, and Sungjoon Choi. Score-based generative modeling through stochastic evolution equations in hilbert spaces. In *Thirty-seventh Conference on Neural Information Processing Systems*, 2023.

[4] Robin Rombach, Andreas Blattmann, Dominik Lorenz, Patrick Esser, and Björn Ommer. High-resolution image synthesis with latent diffusion models. In *Proceedings of the IEEE/CVF conference on computer vision and pattern recognition*, pages 10684–10695, 2022.

[5] Dustin Podell, Zion English, Kyle Lacey, Andreas Blattmann, Tim Dockhorn, Jonas Müller, Joe Penna, and Robin Rombach. SDXL: Improving latent diffusion models for high-resolution image synthesis. In *The Twelfth International Conference on Learning Representations*, 2024.

[6] Aditya Ramesh, Prafulla Dhariwal, Alex Nichol, Casey Chu, and Mark Chen. Hierarchical text-conditional image generation with clip latents. *arXiv preprint arXiv:2204.06125*, 1(2):3, 2022.

[7] William Peebles and Saining Xie. Scalable diffusion models with transformers. In *Proceedings of the IEEE/CVF international conference on computer vision*, pages 4195–4205, 2023.

[8] Omri Avrahami, Dani Lischinski, and Ohad Fried. Blended diffusion for text-driven editing of natural images. In *Proceedings of the IEEE/CVF conference on computer vision and pattern recognition*, pages 18208–18218, 2022.

[9] Bahjat Kawar, Shiran Zada, Oran Lang, Omer Tov, Huiwen Chang, Tali Dekel, Inbar Mosseri, and Michal Irani. Imagic: Text-based real image editing with diffusion models. In *Proceedings of the IEEE/CVF conference on computer vision and pattern recognition*, pages 6007–6017, 2023.

[10] Lvmin Zhang, Anyi Rao, and Maneesh Agrawala. Adding conditional control to text-to-image diffusion models. In *Proceedings of the IEEE/CVF international conference on computer vision*, pages 3836–3847, 2023.

[11] Nataniel Ruiz, Yuanzhen Li, Varun Jampani, Yael Pritch, Michael Rubinstein, and Kfir Aberman. Dreambooth: Fine tuning text-to-image diffusion models for subject-driven generation. In *Proceedings of the IEEE/CVF conference on computer vision and pattern recognition*, pages 22500–22510, 2023.

[12] Jiaming Song, Chenlin Meng, and Stefano Ermon. Denoising diffusion implicit models. *arXiv preprint arXiv:2010.02502*, 2020.

[13] Cheng Lu, Yuhao Zhou, Fan Bao, Jianfei Chen, Chongxuan Li, and Jun Zhu. Dpm-solver: A fast ode solver for diffusion probabilistic model sampling in around 10 steps. *Advances in Neural Information Processing Systems*, 35:5775–5787, 2022.

[14] Yang Song, Prafulla Dhariwal, Mark Chen, and Ilya Sutskever. Consistency models, 2023.

[15] Tim Salimans and Jonathan Ho. Progressive distillation for fast sampling of diffusion models. *arXiv preprint arXiv:2202.00512*, 2022.

[16] Xinyin Ma, Gongfan Fang, and Xinchao Wang. Deepcache: Accelerating diffusion models for free. In *Proceedings of the IEEE/CVF conference on computer vision and pattern recognition*, pages 15762–15772, 2024.

[17] Yu Xu, Fan Tang, Juan Cao, Yuxin Zhang, Xiaoyu Kong, Jintao Li, Oliver Deussen, and Tong-Yee Lee. Headrouter: A training-free image editing framework for mm-dits by adaptively routing attention heads. *arXiv preprint arXiv:2411.15034*, 2024.

[18] Alireza Ganjdanesh, Reza Shirkavand, Shangqian Gao, and Heng Huang. Not all prompts are made equal: Prompt-based pruning of text-to-image diffusion models. In *The Thirteenth International Conference on Learning Representations*, 2025.

[19] Dingkun Zhang, Sijia Li, Chen Chen, Qingsong Xie, and Haonan Lu. Laptop-diff: Layer pruning and normalized distillation for compressing diffusion models. *arXiv preprint arXiv:2404.11098*, 2024.

[20] Thibault Castells, Hyoung-Kyu Song, Bo-Kyeong Kim, and Shinkook Choi. Ld-pruner: Efficient pruning of latent diffusion models using task-agnostic insights, 2024.

[21] Fan Bao, Chongxuan Li, Jun Zhu, and Bo Zhang. Analytic-dpm: an analytic estimate of the optimal reverse variance in diffusion probabilistic models, 2022.

[22] Luping Liu, Yi Ren, Zhijie Lin, and Zhou Zhao. Pseudo numerical methods for diffusion models on manifolds. In *International Conference on Learning Representations*, 2022.

[23] Qinsheng Zhang and Yongxin Chen. Fast sampling of diffusion models with exponential integrator, 2023.

[24] Andy Shih, Suneel Belkhale, Stefano Ermon, Dorsa Sadigh, and Nima Anari. Parallel sampling of diffusion models, 2023.

[25] Simian Luo, Yiqin Tan, Longbo Huang, Jian Li, and Hang Zhao. Latent consistency models: Synthesizing high-resolution images with few-step inference, 2023.

[26] Chenlin Meng, Robin Rombach, Ruiqi Gao, Diederik P. Kingma, Stefano Ermon, Jonathan Ho, and Tim Salimans. On distillation of guided diffusion models, 2023.

[27] Axel Sauer, Dominik Lorenz, Andreas Blattmann, and Robin Rombach. Adversarial diffusion distillation, 2023.

[28] David Berthelot, Arnaud Autef, Jierui Lin, Dian Ang Yap, Shuangfei Zhai, Siyuan Hu, Daniel Zheng, Walter Talbott, and Eric Gu. Tract: Denoising diffusion models with transitive closure time-distillation, 2023.

[29] Zhaoyang Lyu, Xudong XU, Ceyuan Yang, Dahua Lin, and Bo Dai. Accelerating diffusion models via early stop of the diffusion process, 2022.

[30] Haowei Zhu, Dehua Tang, Ji Liu, Mingjie Lu, Jintu Zheng, Jinzhang Peng, Dong Li, Yu Wang, Fan Jiang, Lu Tian, et al. Dip-go: A diffusion pruner via few-step gradient optimization. *Advances in Neural Information Processing Systems*, 37:92581–92604, 2024.

[31] Senmao Li, taihang Hu, Joost van de Weijer, Fahad Khan, Tao Liu, Linxuan Li, Shiqi Yang, Yaxing Wang, Ming-Ming Cheng, and jian Yang. Faster diffusion: Rethinking the role of the encoder for diffusion model inference. In *The Thirty-eighth Annual Conference on Neural Information Processing Systems*, 2024.

[32] Xinyin Ma, Gongfan Fang, Michael Bi Mi, and Xinchao Wang. Learning-to-cache: Accelerating diffusion transformer via layer caching. In *The Thirty-eighth Annual Conference on Neural Information Processing Systems*, 2024.

[33] Felix Wimbauer, Bichen Wu, Edgar Schoenfeld, Xiaoliang Dai, Ji Hou, Zijian He, Artsiom Sanakoyeu, Peizhao Zhang, Sam Tsai, Jonas Kohler, et al. Cache me if you can: Accelerating diffusion models through block caching. In *Proceedings of the IEEE/CVF Conference on Computer Vision and Pattern Recognition*, pages 6211–6220, 2024.

[34] Yuzhang Shang, Zhihang Yuan, Bin Xie, Bingzhe Wu, and Yan Yan. Post-training quantization on diffusion models. In *Proceedings of the IEEE/CVF conference on computer vision and pattern recognition*, pages 1972–1981, 2023.

[35] Junhyuk So, Jungwon Lee, Daehyun Ahn, Hyungjun Kim, and Eunhyeok Park. Temporal dynamic quantization for diffusion models. *Advances in neural information processing systems*, 36:48686–48698, 2023.

[36] Enze Xie, Junsong Chen, Junyu Chen, Han Cai, Haotian Tang, Yujun Lin, Zhekai Zhang, Muyang Li, Ligeng Zhu, Yao Lu, et al. Sana: Efficient high-resolution image synthesis with linear diffusion transformers. *arXiv preprint arXiv:2410.10629*, 2024.

[37] Song Han, Huizi Mao, and William J Dally. Deep compression: Compressing deep neural networks with pruning, trained quantization and huffman coding. *arXiv preprint arXiv:1510.00149*, 2015.

[38] Trevor Gale, Erich Elsen, and Sara Hooker. The state of sparsity in deep neural networks. *arXiv preprint arXiv:1902.09574*, 2019.

[39] Tianyi Chen, Luming Liang, Tianyu Ding, Zhihui Zhu, and Ilya Zharkov. Otov2: Automatic, generic, user-friendly. *arXiv preprint arXiv:2303.06862*, 2023.

[40] Runxue Bao, Bin Gu, and Heng Huang. An accelerated doubly stochastic gradient method with faster explicit model identification. In *Proceedings of the 31st ACM International Conference on Information & Knowledge Management*, pages 57–66, 2022.

[41] Runxue Bao, Xidong Wu, Wenhan Xian, and Heng Huang. Doubly sparse asynchronous learning for stochastic composite optimization. In *Thirty-First International Joint Conference on Artificial Intelligence (IJCAI)*, pages 1916–1922, 2022.

[42] Shangqian Gao, Zeyu Zhang, Yanfu Zhang, Feihu Huang, and Heng Huang. Structural alignment for network pruning through partial regularization. In *Proceedings of the IEEE/CVF International Conference on Computer Vision (ICCV)*, pages 17402–17412, October 2023.

[43] Shangqian Gao, Junyi Li, Zeyu Zhang, Yanfu Zhang, Weidong Cai, and Heng Huang. Device-wise federated network pruning. In *Proceedings of the IEEE/CVF Conference on Computer Vision and Pattern Recognition (CVPR)*, pages 12342–12352, June 2024.

[44] Xin Dong, Shangyu Chen, and Sinno Jialin Pan. Learning to prune deep neural networks via layer-wise optimal brain surgeon, 2017.

[45] Sejun Park, Jaeho Lee, Sangwoo Mo, and Jinwoo Shin. Lookahead: A far-sighted alternative of magnitude-based pruning, 2020.

[46] Elias Frantar and Dan Alistarh. Sparsegpt: Massive language models can be accurately pruned in one-shot. In *International Conference on Machine Learning*, pages 10323–10337. PMLR, 2023.

[47] Mingyang Zhang, Hao Chen, Chunhua Shen, Zhen Yang, Linlin Ou, Xinyi Yu, and Bohan Zhuang. Loraprune: Pruning meets low-rank parameter-efficient fine-tuning. *arXiv preprint arXiv:2305.18403*, 2023.

[48] Saleh Ashkboos, Maximilian L Croci, Marcelo Gennari do Nascimento, Torsten Hoefler, and James Hensman. Slicegpt: Compress large language models by deleting rows and columns. In *The Twelfth International Conference on Learning Representations*, 2024.

[49] Gongfan Fang, Xinyin Ma, and Xinchao Wang. Structural pruning for diffusion models. In *Thirty-seventh Conference on Neural Information Processing Systems*, 2023.

[50] Yanyu Li, Huan Wang, Qing Jin, Ju Hu, Pavlo Chemerys, Yun Fu, Yanzhi Wang, Sergey Tulyakov, and Jian Ren. Snapfusion: Text-to-image diffusion model on mobile devices within two seconds. *Advances in Neural Information Processing Systems*, 36:20662–20678, 2023.

[51] Xingyi Yang, Daquan Zhou, Jiashi Feng, and Xinchao Wang. Diffusion probabilistic model made slim, 2022.

[52] Xidong Wu, Shangqian Gao, Zeyu Zhang, Zhenzhen Li, Runxue Bao, Yanfu Zhang, Xiaoqian Wang, and Heng Huang. Auto-train-once: Controller network guided automatic network pruning from scratch. In *Proceedings of the IEEE/CVF Conference on Computer Vision and Pattern Recognition (CVPR)*, pages 16163–16173, June 2024.

[53] Bo-Kyeong Kim, Hyoung-Kyu Song, Thibault Castells, and Shinkook Choi. Bk-sdm: A lightweight, fast, and cheap version of stable diffusion. *arXiv preprint arXiv:2305.15798*, 2023.

[54] Wangbo Zhao, Yizeng Han, Jiasheng Tang, Kai Wang, Yibing Song, Gao Huang, Fan Wang, and Yang You. Dynamic diffusion transformer. In *The Thirteenth International Conference on Learning Representations*, 2025.

[55] Nan Du, Yanping Huang, Andrew M Dai, Simon Tong, Dmitry Lepikhin, Yuanzhong Xu, Maxim Krikun, Yanqi Zhou, Adams Wei Yu, Orhan Firat, et al. Glam: Efficient scaling of language models with mixture-of-experts. In *International Conference on Machine Learning*, pages 5547–5569. PMLR, 2022.

[56] Albert Q Jiang, Alexandre Sablayrolles, Antoine Roux, Arthur Mensch, Blanche Savary, Chris Bamford, Devendra Singh Chaplot, Diego de las Casas, Emma Bou Hanna, Florian Bressand, et al. Mixtral of experts. *arXiv preprint arXiv:2401.04088*, 2024.

[57] Junmo Kang, Leonid Karlinsky, Hongyin Luo, Zhen Wang, Jacob Hansen, James Glass, David Cox, Rameswar Panda, Rogerio Feris, and Alan Ritter. Self-moe: Towards compositional large language models with self-specialized experts, 2024.

[58] Shangqian Gao, Ting Hua, Reza Shirkavand, Chi-Heng Lin, Zhen Tang, Zhengao Li, Longge Yuan, Fangyi Li, Zeyu Zhang, Alireza Ganjdanesh, Lou Qian, Xu Jie, and Yen-Chang Hsu. To-moe: Converting dense large language models to mixture-of-experts through dynamic structural pruning, 2025.

[59] Alireza Ganjdanesh, Yan Kang, Yuchen Liu, Richard Zhang, Zhe Lin, and Heng Huang. Mixture of efficient diffusion experts through automatic interval and sub-network selection. In *European Conference on Computer Vision*, pages 54–71. Springer, 2024.

[60] Haotian Sun, Tao Lei, Bowen Zhang, Yanghao Li, Haoshuo Huang, Ruoming Pang, Bo Dai, and Nan Du. EC-DIT: Scaling diffusion transformers with adaptive expert-choice routing. In *The Thirteenth International Conference on Learning Representations*, 2025.

[61] Ashish Vaswani, Noam Shazeer, Niki Parmar, Jakob Uszkoreit, Llion Jones, Aidan N Gomez, Łukasz Kaiser, and Illia Polosukhin. Attention is all you need. *Advances in neural information processing systems*, 30, 2017.

[62] Olaf Ronneberger, Philipp Fischer, and Thomas Brox. U-net: Convolutional networks for biomedical image segmentation. In *Medical image computing and computer-assisted intervention–MICCAI 2015: 18th international conference, Munich, Germany, October 5-9, 2015, proceedings, part III 18*, pages 234–241. Springer, 2015.

[63] Prafulla Dhariwal and Alexander Nichol. Diffusion models beat gans on image synthesis. *Advances in neural information processing systems*, 34:8780–8794, 2021.

[64] Eric Jang, Shixiang Gu, and Ben Poole. Categorical reparameterization with gumbel-softmax. *arXiv preprint arXiv:1611.01144*, 2016.

[65] Dmitry Lepikhin, HyoukJoong Lee, Yuanzhong Xu, Dehao Chen, Orhan Firat, Yanping Huang, Maxim Krikun, Noam Shazeer, and Zhifeng Chen. {GS}hard: Scaling giant models with conditional computation and automatic sharding. In *International Conference on Learning Representations*, 2021.

[66] William Fedus, Barret Zoph, and Noam Shazeer. Switch transformers: Scaling to trillion parameter models with simple and efficient sparsity. *Journal of Machine Learning Research*, 23(120):1–39, 2022.

[67] Christoph Schuhmann, Romain Beaumont, Richard Vencu, Cade Gordon, Ross Wightman, Mehdi Cherti, Theo Coombes, Aarush Katta, Clayton Mullis, Mitchell Wortsman, et al. Laion-5b: An open large-scale dataset for training next generation image-text models. *Advances in neural information processing systems*, 35:25278–25294, 2022.

[68] Piyush Sharma, Nan Ding, Sebastian Goodman, and Radu Soricut. Conceptual captions: A cleaned, hypernymed, image alt-text dataset for automatic image captioning. In *Proceedings of the 56th Annual Meeting of the Association for Computational Linguistics (Volume 1: Long Papers)*, pages 2556–2565, 2018.

[69] Tsung-Yi Lin, Michael Maire, Serge Belongie, James Hays, Pietro Perona, Deva Ramanan, Piotr Dollár, and C Lawrence Zitnick. Microsoft coco: Common objects in context. In *Computer vision–ECCV 2014: 13th European conference, zurich, Switzerland, September 6-12, 2014, proceedings, part v 13*, pages 740–755. Springer, 2014.

[70] Martin Heusel, Hubert Ramsauer, Thomas Unterthiner, Bernhard Nessler, and Sepp Hochreiter. Gans trained by a two time-scale update rule converge to a local nash equilibrium. *Advances in neural information processing systems*, 30, 2017.

[71] Sadeep Jayasumana, Srikumar Ramalingam, Andreas Veit, Daniel Glasner, Ayan Chakrabarti, and Sanjiv Kumar. Rethinking fid: Towards a better evaluation metric for image generation. In *Proceedings of the IEEE/CVF Conference on Computer Vision and Pattern Recognition*, pages 9307–9315, 2024.

[72] Jack Hessel, Ari Holtzman, Maxwell Forbes, Ronan Le Bras, and Yejin Choi. Clipscore: A reference-free evaluation metric for image captioning. *arXiv preprint arXiv:2104.08718*, 2021.

[73] Gongfan Fang, Kunjun Li, Xinyin Ma, and Xinchao Wang. Tinyfusion: Diffusion transformers learned shallow. *arXiv preprint arXiv:2412.01199*, 2024.

[74] Jia Deng, Wei Dong, Richard Socher, Li-Jia Li, Kai Li, and Li Fei-Fei. Imagenet: A large-scale hierarchical image database. In *2009 IEEE conference on computer vision and pattern recognition*, pages 248–255. Ieee, 2009.

[75] Yoshua Bengio, Nicholas Léonard, and Aaron Courville. Estimating or propagating gradients through stochastic neurons for conditional computation. *arXiv preprint arXiv:1308.3432*, 2013.

[76] Ilya Loshchilov and Frank Hutter. Decoupled weight decay regularization. In *International Conference on Learning Representations*, 2019.

[77] Jonathan Ho and Tim Salimans. Classifier-free diffusion guidance. *arXiv preprint arXiv:2207.12598*, 2022.

[78] Jiazheng Xu, Xiao Liu, Yuchen Wu, Yuxuan Tong, Qinkai Li, Ming Ding, Jie Tang, and Yuxiao Dong. Imagereward: Learning and evaluating human preferences for text-to-image generation. *Advances in Neural Information Processing Systems*, 36:15903–15935, 2023.

[79] Xiaoshi Wu, Yiming Hao, Keqiang Sun, Yixiong Chen, Feng Zhu, Rui Zhao, and Hongsheng Li. Human preference score v2: A solid benchmark for evaluating human preferences of text-to-image synthesis. *arXiv preprint arXiv:2306.09341*, 2023.

[80] Daniel Bolya and Judy Hoffman. Token merging for fast stable diffusion. In *Proceedings of the IEEE/CVF conference on computer vision and pattern recognition*, pages 4599–4603, 2023.

A Limitations

While ALTER employs joint optimization for the co-adaptation of the U-Net and hypernetwork, a final fine-tuning stage for the dynamically pruned U-Net is still found to be a necessary step after T_{end} is reached. This final tuning phase is crucial for fully recovering any potential performance degradation incurred during the temporal-wise structure pruning and for allowing the U-Net to optimally adapt to its newly defined sparse, dynamic structure, thereby maximizing its generative quality.

B More Details of ALTER

This appendix provides further details on the architectural components of our hypernetwork $\boldsymbol{H}_\Phi$, the calculation of sparsity metrics, the implementation of Gumbel-Sigmoid and Gumbel-Softmax with straight-through estimation, and the handling of dynamic masks.

B.1 Detailed Hypernetwork Architectures

The hypernetwork $\boldsymbol{H}_\Phi$ consists of two main modules: the Expert Structure Generator and the Temporal Router. Their architectures are detailed in Table 5 and Table 6. We use D_{input} for the dimensionality of the learnable embeddings for the Expert Structure Generator, D_{expert} for its hidden layer, D_{emb} for the UNet's timestep embedding dimension, and D_{router} for the Temporal Router's hidden layer. Specific values used in our experiments are provided in Appendix C.

Table 5: Architecture of the Expert Structure Generator module in $\boldsymbol{H}_\Phi$. Processes $N_e \times N_L$ input embeddings to produce $N_e \times N_L$ logits.

Component	**Details**
Input	Frozen Embeddings $Z \in \mathbb{R}^{N_e \times N_L \times D_{\text{input}}}$ (Initialized orthogonally)
Hidden Layer	Linear($D_{\text{input}} \to D_{\text{expert}}$) $\to$ LayerNorm(D_{expert}) $\to$ ReLU
Output Layer	Linear($D_{\text{expert}} \to 1$, no bias)
Output	Logits $L_{\text{experts}} \in \mathbb{R}^{N_e \times N_L}$ (Squeeze last dim)

Table 6: Architecture of the Temporal Router module ($\boldsymbol{R}_{\text{router}}$) in $\boldsymbol{H}_\Phi$. Processes each timestep embedding e_t to produce N_e routing logits.

Component	**Details**
Input	Timestep Embedding $e_t \in \mathbb{R}^{D_{emb}}$ (from $E_{\text{timesteps}} \in \mathbb{R}^{T_{\text{total}} \times D_{emb}}$)
Hidden Layer	Linear($D_{emb} \to D_{\text{router}}$) $\to$ LayerNorm(D_{router}) $\to$ ReLU
Output Layer	Linear($D_{\text{router}} \to N_e$, no bias)
Output	Routing Logits $L_t^{\text{routing}} \in \mathbb{R}^{N_e}$ (for a single e_t) (Total output $L^{\text{routing}} \in \mathbb{R}^{T_{\text{total}} \times N_e}$)

B.2 Calculation of Current Sparsity

The current effective sparsity $S(m'_t)$ used in the sparsity regularization term $\mathcal{L}_{\text{ratio}}$ (Equation 5), quantifies the active computational cost relative to the total potential cost. It is calculated based on the soft (differentiable) pruning masks m'_t generated by $\boldsymbol{H}_\Phi$ during its training phase. Let $(m'_t)_l$ be the soft mask value for the l-th prunable layer and c_l be the pre-calculated computational cost (e.g., FLOPs) of that layer. The current sparsity $S(m'_t)$ is the weighted average of these mask values, normalized by the total cost of all prunable layers:

$$S(m'_t) = \frac{\sum_{l=1}^{N_L} (m'_t)_l \cdot c_l}{\sum_{l=1}^{N_L} c_l} \tag{8}$$

This formulation ensures that $S(m'_t)$ represents the fraction of the total computational cost that remains active under the current soft mask m'_t. The per-layer costs c_l are typically profiled once from the pretrained full UNet architecture.

B.3 ST-GS & ST-GSmax Implementation Details

To enable differentiable sampling of discrete architectural decisions, we employ ST-GS and ST-GSMax techniques.

ST-GS Sampling. For layer pruning decisions within the Expert Structure Generator, logits $(L_{\text{experts}})_{e,l}$ are converted to binary masks. We sample Gumbel noise $g \sim \text{Gumbel}(0, 1)$. Given a logit L, a sampling temperature $\tau_g = 0.4$, and an offset $b_g = 4$, the soft decision y_g is computed:

$$y_g = \sigma\left(\frac{L + g + b_g}{\tau_g}\right)$$

where $\sigma(\cdot)$ is the sigmoid function. To obtain a hard binary decision $(M_{\text{experts}})_{e,l}$ while maintaining differentiability for training, we use STE [75]: $(M_{\text{experts}})_{e,l} = \text{round}(y_g)$. During backpropagation, the gradient is passed through y_g as if the rounding operation were the identity function for values not exactly at 0.5, effectively using $\nabla(\text{round}(y_g)) \approx \nabla y_g$. This results in a tensor of '0's and '1's for the forward pass, forming the pruning masks.

ST-GSmax Sampling. For temporal routing decisions, given a vector of routing logits $L_t^{\text{routing}} \in \mathbb{R}^{N_e}$, a temperature $\tau_r = 0.4$, an offset $b_r = 0$, and a vector of Gumbel noise $\boldsymbol{G} \in \mathbb{R}^{N_e}$ (components g_j sampled independently), the soft Gumbel-Softmax probabilities $y_r \in [0, 1]^{N_e}$ are:

$$(y_r)_j = \frac{\exp(((L_t^{\text{routing}})_j + g_j + b_r)/\tau_r)}{\sum_{k=1}^{N_e} \exp(((L_t^{\text{routing}})_k + g_k + b_r)/\tau_r)}$$

To obtain a hard one-hot selection vector s_t for the forward pass while enabling gradient flow for training, STE is applied. Determine the index of the maximally activated expert: $j^* = \text{argmax}_j(y_r)_j$. Create a hard one-hot vector $(s_t^{\text{hard}})_j = \mathbf{1}_{j=j^*}$. The output used in computation, which enables STE, is $s_t = (s_t^{\text{hard}} - y_r).\text{detach}() + y_r$. This makes s_t a one-hot vector in the forward pass, while its gradient in the backward pass is taken with respect to the soft probabilities y_r.

B.4 Dynamic Mask Handling

The dynamic pruning masks, central to ALTER's efficiency, are generated and applied as follows. For each timestep t, an effective mask $m_t \in [0, 1]^{N_L}$ is composed from the N_e expert structure masks M_{experts} and the per-timestep routing selection s_t. When training the UNet or during inference, deterministic binary masks (m_t^{hard}, forming the set $\mathcal{M}_{\text{UNet}}$) are derived by setting the hypernetwork $\boldsymbol{H}_\Phi$ to evaluation mode. For training $\boldsymbol{H}_\Phi$ itself, differentiable soft versions of these masks (m'_t) are utilized.

The UNet architecture has a specific block structure. The generated flat mask vector (whether m_t^{hard} or m'_t) of length N_L is mapped to the corresponding prunable layers within the UNet using a utility function. This ensures that the correct mask component $(m_t)_l$ is applied to the l-th prunable layer f_l. The application of this component follows Equation 2 from the main text: $x_{\text{out}} = (1 - (m_t)_l) \cdot x_{\text{in}} + (m_t)_l \cdot f_l(x_{\text{in}})$. This general mechanism applies to all designated prunable layers. It is noteworthy that in UNet architectures, particularly in the decoder pathway, layers f_l often process inputs that are a result of concatenating features from a previous layer in the same pathway with features from an earlier encoder layer via a skip connection. Our layer-wise pruning applies directly to such layers f_l: if f_l is skipped due to $(m_t)_l \approx 0$, its entire operation, including its specific handling of any skip-connected features, is bypassed.

C More Implementation Details

Here we provide additional details regarding our experimental setup, training details and hyperparameter configurations for ALTER. All models are trained or fine-tuned starting from official pretrained

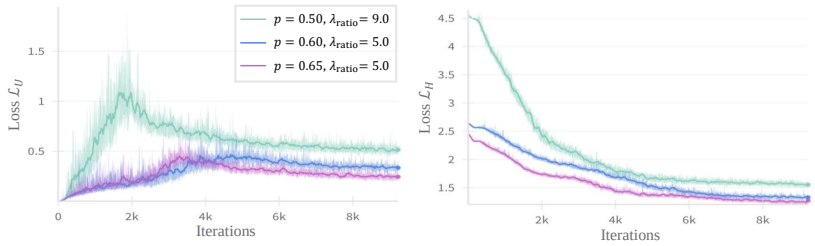

(a) Loss $\mathcal{L}_U$ (b) Loss $\mathcal{L}_H$

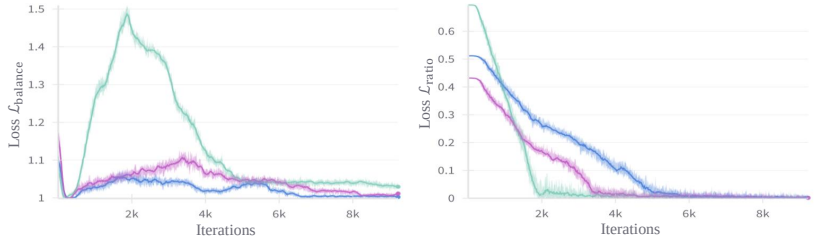

(c) Loss $\mathcal{L}_{\text{balance}}$ (d) Loss $\mathcal{L}_{\text{ratio}}$

Figure 5: The training dynamics given different ratios p and λ_{ratio} weights.

SD-2.1 [4] checkpoints. The training is conducted at a resolution of 512×512 pixels using a randomly sampled subset of 0.3M images from the LAION-Aesthetics V2 dataset (rated 6.5+) [67]. The total optimization process spans $T = 32,000$ steps with a global batch size of 64, distributed across 2 A100 GPUs (32 samples per GPU). The hypernetwork $\boldsymbol{H}_\Phi$ is actively trained until T_{end}, which is set to 2 epochs. We employ $N_e = 10$ temporal experts and sparsity ratio $p = 0.65$ for our main experiments. We use the AdamW optimizer [76] for both the U-Net parameters θ and the hypernetwork parameters Φ. A linear learning rate warm-up is applied for the first 250 iterations for both optimizers. After the warm-up phase, constant learning rates are used: 1×10^{-5} for the U-Net and 7×10^{-5} for the hypernetwork. For the GS function used in the Expert Generator, the temperature τ_g is set to 0.4 and the offset b_g to 4.0, which initializes expert masks to all-ones, promoting layer activity at the start of training and preventing an overly detrimental impact on the U-Net from aggressive initial pruning. For the GSmax function in the Temporal Router, the temperature τ_r is 0.4 and the offset b_r is 0.0. Since the denoising loss L_{denoise} tends to result in unstable optimization and slow convergence. The loss weights for the objective functions are set to $\lambda_{\text{denoise}} = 1e-4$, $\lambda_{\text{outKD}} = \lambda_{\text{featKD}} = \lambda_{\text{balance}=1.0}$ and $\lambda_{\text{ratio}} = 5.0$. For hypernetwork's implementation, we set $D_{\text{input}} = 64$, $D_{\text{expert}} = 256$, $D_{\text{router}} = 64$, and the D_{emb} is depedent on the pre-trained official SDv2.1 model. For generating samples for evaluation, we use classifier-free guidance (CFG) [77] with the default scale of the respective SDv2.1 checkpoint (e.g., 7.5). Image generation is performed using the PNDM sampler [22], following practices in prior works for consistency.

D More Experimental Results

D.1 Training Dynamics

In Fig. 5, we visualize the training dynamics for different pruning ratios p and their associated λ_{ratio}, highlighting the co-adaptation between the shared UNet backbone and the hypernetwork. As shown in Fig. 5(a), the UNet loss $\mathcal{L}_U$ generally follows a two-phase pattern: it first increases, especially under high sparsity targets (e.g., $p = 0.50$), and then gradually decreases. This early rise reflects a transient mismatch, as the hypernetwork begins to sample diverse pruning structures across timesteps while the shared UNet parameters have not yet adapted to the corresponding architectural variations. Over time, however, $\mathcal{L}_U$ steadily declines, indicating that the shared UNet progressively learns to meet the performance demands imposed by a wide range of expert sub-structure configurations at different timesteps. The final converged $\mathcal{L}_U$ remains slightly higher under more aggressive pruning configurations, reflecting the expected trade-off between model sparsity and generative fidelity.

Table 7: Comparison of Image Reward and HPSv2 metrics. The images are sampled with 25-step inference.

Method	**MACs**(G)(↓)	**Image Reward**(↑)	**HPSv2**(↑)
SDv2.1	1384.2	0.1139	24.47
BK-SDM-v2-Base	876.5	-0.0365	23.97
APTP (0.66) (COCO)	916.3	-0.8706	19.08
APTP (0.66) (CC3M)	916.3	-1.2226	18.19
ALTER (0.65) (Ours)	899.7	0.1494	24.54
ALTER (0.60) (Ours)	830.5	0.1487	24.36

Table 8: Comparison of SSIM and PSNR metrics.

Method	**Steps**	**MACs** (G)(↓)	**Latency** (s)(↑)	**CC3M**		**MS-COCO**	
				SSIM (↑)	**PSNR** (↑)	**SSIM** (↑)	**PSNR** (↑)
SDv2.1	25	1384.2	4.0	-	-	-	-
SDv2.1	20	1384.2	3.2	0.3529	13.71	0.1582	10.24
BK-SDM-v2 (Base)	25	876.5	2.5	0.1208	9.42	0.1551	9.47
APTP (0.66)	25	916.3	2.6	0.0782	8.99	0.0730	8.83
ALTER (0.65) (Ours)	25	899.7	2.6	0.1233	9.90	0.3261	12.81
ALTER (0.65) (Ours)	20	899.7	2.1	0.1247	9.95	0.2484	11.61
ALTER (0.60) (Ours)	20	830.5	1.9	0.1224	9.94	0.1898	10.73

In contrast, the hypernetwork's loss $\mathcal{L}_H$ (Fig. 5(b)) exhibits a steady and consistent decline across all configurations, indicating that $\boldsymbol{H}_\Phi$ is effectively optimizing its composite objective, which includes the UNet performance term $\mathcal{L}_{\text{perf}}$ and the associated regularization components. This consistent improvement suggests that the hypernetwork progressively discovers better expert structures and routing strategies alongside the UNet's parameter update, while gradually approaching the desired computational reduction target.

The regularization losses further elucidate this process. The sparsity loss $\mathcal{L}_{\text{ratio}}$ (Fig. 5(d)) decreases smoothly over time, confirming that the hypernetwork successfully aligns the average computational cost of selected experts with the target sparsity level p. The convergence rate is influenced by both the sparsity target and the loss weight λ_{ratio}. Similarly, the router balance loss $\mathcal{L}_{\text{balance}}$ (Fig. 5(c)) shows a downward trend, indicating that the temporal router gradually learns to distribute computation evenly across experts. Notably, under the most aggressive pruning setting ($p = 0.50$), $\mathcal{L}_{\text{balance}}$ initially spikes, suggesting a greater challenge in achieving balanced routing when sparsity constraints are tighter.

This intricate interplay—where $\mathcal{L}_H$ steadily improves while $\mathcal{L}_U$ undergoes a transient perturbation—highlights the bi-level nature of ALTER's optimization process, which enables the emergence of efficient, dynamically structured expert configurations.

This intricate interplay, where $\mathcal{L}_H$ steadily improves while $\mathcal{L}_U$ overcomes an initial perturbation, highlights the bi-level nature of the optimization problem that ALTER navigates to achieve its efficient, dynamically structured experts with high performance preservation.

D.2 More Evaluation Metrics

ImageReward and HPSv2 We benchmark our models using advanced preference metrics, ImageReward [78] and Human Preference Score v2 (HPSv2) [79] in order to provide a more comprehensive evaluation of generation quality. These metrics assess perceptual quality and human aesthetic preference. As shown om Table 7, our method ranks highest on both metrics, even outperforming the original SDv2.1, confirming that our efficiency gains do not come at the cost of visual quality.

SSIM and PSNR We provide the SSIM and PSNR to show the deviation of different methods from the original SDv2.1 25-step inference. As shown in Table 8, our method ALTER not only matches the MACs of prior work but also achieves significantly higher SSIM and PSNR scores,

Table 9: Scalability with token reduction method ToMeSD on the MS-COCO 2017 validation set.

Method	Steps	ToMe r%	Speedup(↑)	CLIP (↑)	FID-5K (↓)
SDv2.1	50	0	1.00×	31.55	27.29
SDv2.1	20	0	2.49×	31.53	27.83
ALTER (0.65) (Ours)	20	0	3.64×	31.62	25.25
w/ ToMeSD [80]	20	40	4.93×	31.48	25.93
	20	50	5.75×	31.34	26.89
	20	60	6.54×	31.24	27.96

Table 10: Ablation study on the sparsity ratio p. The images are sampled with 20-step inference.

Method	CC3M					MS-COCO				
	MACs (G)(↓)	Latency (s)(↓)	FID (↓)	CLIP (↑)	CMMD (↓)	MACs (G)(↓)	Latency (s) (↓)	FID (↓)	CLIP (↑)	CMMD (↓)
SDv2.1 [4]	1384.2	3.2	17.37	30.89	0.374	1384.2	3.2	14.46	32.08	0.532
ALTER (0.65)	899.7	2.1	17.14	30.92	0.392	899.7	2.1	13.89	32.18	0.533
ALTER (0.60)	830.5	1.9	17.87	30.88	0.479	830.5	1.9	14.24	32.17	0.596
ALTER (0.55)	761.3	1.8	18.27	30.87	0.563	761.3	1.8	14.59	32.16	0.679
ALTER (0.50)	692.1	1.6	18.99	30.74	0.612	692.1	1.6	14.70	32.05	0.727

which demonstrates that our approach better preserves the generative characteristics of the original model.

D.3 Generality to DiT

To assess generality beyond U-Nets, we apply *ALTER* to a DiT-XL/2 backbone [7] and evaluate on ImageNet [74] at 256×256 using a 250-step DDPM sampler [2].

As shown in Table 4, our method achieves a $1.92\times$ speedup while maintaining an FID score (2.36) comparable to the full model (2.27). With approximately half the layers active on average, our method significantly outperforms static pruning (TinyFusion [73]), especially on key quality metrics like IS (254.29 vs. 234.50) and FID (2.36 vs. 2.86). When comparing to dynamic methods like DyDiT [54], ALTER brings higher speedup. It is important to note that our approaches are orthogonal and complementary. ALTER performs coarse-grained layer-level pruning, while DyDiT performs fine-grained pruning within each block. This empirically confirms that our framework is effective beyond U-Nets and is applicable to modern Transformer-based architectures.

D.4 Scalability with Other Accelerators

ALTER's design makes it orthogonal to and compatible with other diffusion acceleration methods such as diffusion cache and token reduction. We conduct an experiment combining ALTER with a token reduction method ToMeSD [80] to demonstrate ALTER's scalability. For this combination, we follow the default setting of ToMeSD. As shown in Table 9, we boost the total speedup from $3.64\times$ to an impressive $6.54\times$ with only a minor, controllable trade-off in performance scores. This empirically validates the excellent scalability of our method.

D.5 Ablation Study of Sparsity Ratio

We investigate the impact of varying the target sparsity ratio p on ALTER's performance. Results are reported in Table 10 under the unified 20-step inference setting, showing a clear trade-off between sparsity and generation quality. As p decreases from 0.65 to 0.50, performance metrics degrade gradually. Notably, ALTER variants with $p = 0.65$ and $p = 0.60$ match the generative quality of the original SDv2.1 baseline while significantly reducing computational cost. Even the most aggressive setting, ALTER (0.50), maintains competitive performance (e.g., FID of 14.70 and CLIP score of 32.05 on MS-COCO) with the highest efficiency gains. These results highlight ALTER's flexibility and its ability to balance quality and efficiency under different sparsity budgets.

Table 11: Ablation study on different components of $\mathcal{L}_U$ for the "Static" Variant.

$\mathcal{L}_U$	CC3M			MS-COCO		
	FID (↓)	**CLIP** (↑)	**CMMD** (↓)	**FID** (↓)	**CLIP** (↑)	**CMMD** (↓)
$\mathcal{L}_{\text{denoise}}$	23.76	29.93	0.531	21.57	30.91	0.709
$\mathcal{L}_{\text{denoise}} + \mathcal{L}_{\text{outKD}}$	20.15	30.54	0.424	15.98	31.79	0.549
$\mathcal{L}_{\text{denoise}} + \mathcal{L}_{\text{outKD}} + \mathcal{L}_{\text{featKD}}$	**19.03**	**30.75**	**0.397**	**15.35**	**32.01**	**0.544**

Table 12: Ablation of post-T_{end} fine-tuning.

Method	**Steps**	**CLIP**(↑)	**FID-5K**(↓)
SDv2.1	20	31.53	27.83
ALTER (0.65) (T_{end})	20	31.54	25.98
ALTER (0.65) (T_{total})	20	31.62	25.25
ALTER (0.65) (T_{end})	15	31.05	27.16
ALTER (0.65) (T_{total})	15	31.19	26.58

D.6 Ablation on Loss Components of $\mathcal{L}_U$

We investigate the impact of incorporating knowledge distillation losses into the UNet's training objective $\mathcal{L}_U$ for the "Static" variant. As shown in Table 11, introducing the distillation of the output and block features are able to enhance the performance of the statically pruned model, which guides our choice of loss components.

D.7 Ablation on Final Finetuning

As the results in Table 12 demonstrate, the model's performance after T_{end} is already very strong, achieving the majority of the final quality. The final fine-tuning provides a consistent and important boost across both metrics and step counts, further improving both FID and CLIP scores.

D.8 More Qualitative Results

We provide more qualitative results compared with the 25-step original SDv2.1 and BK-SDM-V2-Small. As shown in Fig. 6, ALTER exhibits a quality comparable to the unpruned SD-v2.1 model and displays fewer artifacts than those produced by BK-SDM-v2.

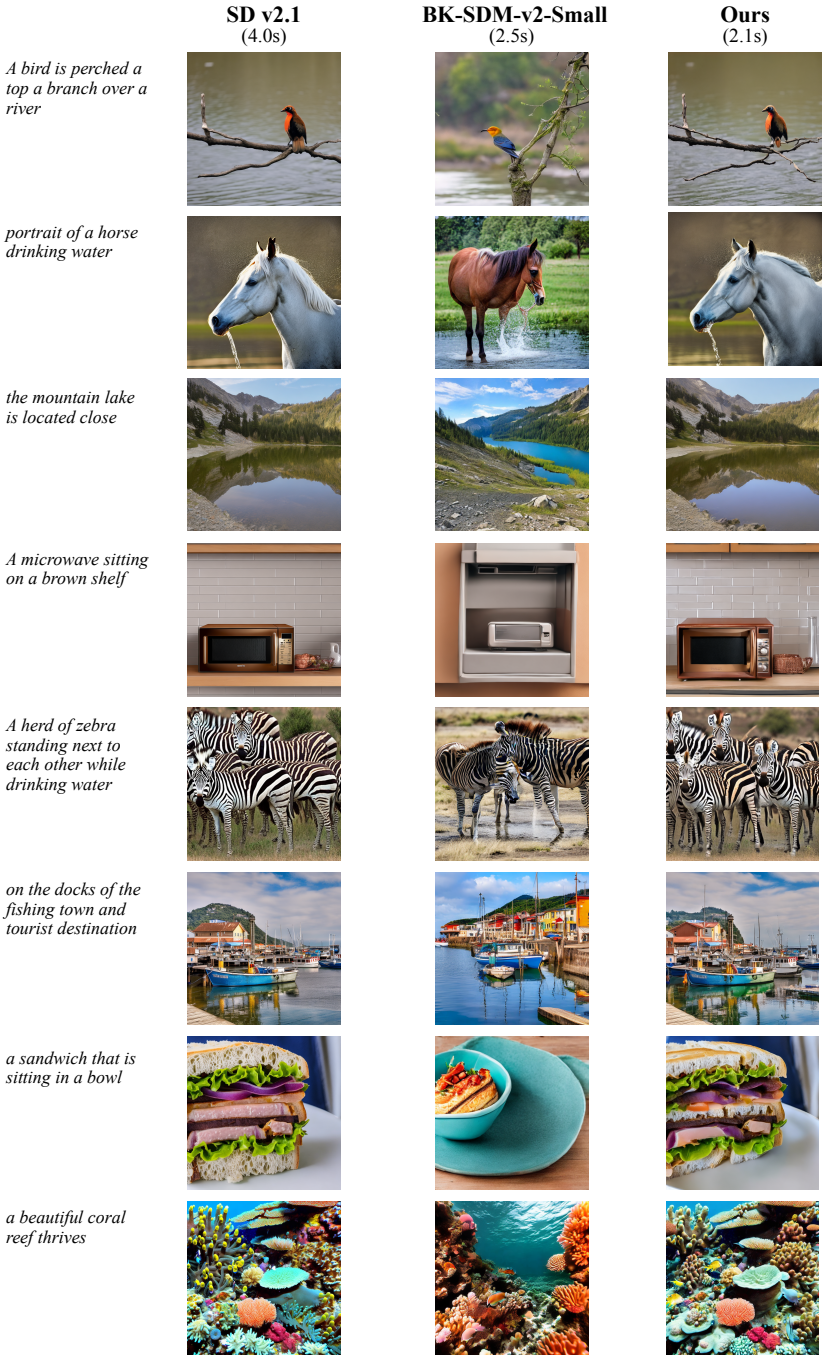

Figure 6: More qualitative results compared with original SDv2.1 and BK-SDM-Small. SDv2.1 and BK-SDM-Small adopt the 25-step PNDM while our method adopts the 20-step inference.

NeurIPS Paper Checklist

1. **Claims**

   Question: Do the main claims made in the abstract and introduction accurately reflect the paper's contributions and scope?

   Answer: [Yes]

   Justification: The abstract and introduction clearly reflect the main contributions and scope of the paper.

   Guidelines:

   - The answer NA means that the abstract and introduction do not include the claims made in the paper.
   - The abstract and/or introduction should clearly state the claims made, including the contributions made in the paper and important assumptions and limitations. A No or NA answer to this question will not be perceived well by the reviewers.
   - The claims made should match theoretical and experimental results, and reflect how much the results can be expected to generalize to other settings.
   - It is fine to include aspirational goals as motivation as long as it is clear that these goals are not attained by the paper.

2. **Limitations**

   Question: Does the paper discuss the limitations of the work performed by the authors?

   Answer: [Yes]

   Justification: We have discussed the limitations of our work. Please refer to Appendix A.

   Guidelines:

   - The answer NA means that the paper has no limitation while the answer No means that the paper has limitations, but those are not discussed in the paper.
   - The authors are encouraged to create a separate "Limitations" section in their paper.
   - The paper should point out any strong assumptions and how robust the results are to violations of these assumptions (e.g., independence assumptions, noiseless settings, model well-specification, asymptotic approximations only holding locally). The authors should reflect on how these assumptions might be violated in practice and what the implications would be.
   - The authors should reflect on the scope of the claims made, e.g., if the approach was only tested on a few datasets or with a few runs. In general, empirical results often depend on implicit assumptions, which should be articulated.
   - The authors should reflect on the factors that influence the performance of the approach. For example, a facial recognition algorithm may perform poorly when image resolution is low or images are taken in low lighting. Or a speech-to-text system might not be used reliably to provide closed captions for online lectures because it fails to handle technical jargon.
   - The authors should discuss the computational efficiency of the proposed algorithms and how they scale with dataset size.
   - If applicable, the authors should discuss possible limitations of their approach to address problems of privacy and fairness.
   - While the authors might fear that complete honesty about limitations might be used by reviewers as grounds for rejection, a worse outcome might be that reviewers discover limitations that aren't acknowledged in the paper. The authors should use their best judgment and recognize that individual actions in favor of transparency play an important role in developing norms that preserve the integrity of the community. Reviewers will be specifically instructed to not penalize honesty concerning limitations.

3. **Theory assumptions and proofs**

   Question: For each theoretical result, does the paper provide the full set of assumptions and a complete (and correct) proof?

   Answer: [NA] .

Justification: Our propositions are mainly based on experiments and empirical results which do not include theoretical results.

Guidelines:

- The answer NA means that the paper does not include theoretical results.
- All the theorems, formulas, and proofs in the paper should be numbered and cross-referenced.
- All assumptions should be clearly stated or referenced in the statement of any theorems.
- The proofs can either appear in the main paper or the supplemental material, but if they appear in the supplemental material, the authors are encouraged to provide a short proof sketch to provide intuition.
- Inversely, any informal proof provided in the core of the paper should be complemented by formal proofs provided in appendix or supplemental material.
- Theorems and Lemmas that the proof relies upon should be properly referenced.

4. **Experimental result reproducibility**

   Question: Does the paper fully disclose all the information needed to reproduce the main experimental results of the paper to the extent that it affects the main claims and/or conclusions of the paper (regardless of whether the code and data are provided or not)?

   Answer: [Yes]

   Justification: We have provided all the implementation details of model design, network training and inference in Section 4.1 and Appendix C.

   Guidelines:

   - The answer NA means that the paper does not include experiments.
   - If the paper includes experiments, a No answer to this question will not be perceived well by the reviewers: Making the paper reproducible is important, regardless of whether the code and data are provided or not.
   - If the contribution is a dataset and/or model, the authors should describe the steps taken to make their results reproducible or verifiable.
   - Depending on the contribution, reproducibility can be accomplished in various ways. For example, if the contribution is a novel architecture, describing the architecture fully might suffice, or if the contribution is a specific model and empirical evaluation, it may be necessary to either make it possible for others to replicate the model with the same dataset, or provide access to the model. In general. releasing code and data is often one good way to accomplish this, but reproducibility can also be provided via detailed instructions for how to replicate the results, access to a hosted model (e.g., in the case of a large language model), releasing of a model checkpoint, or other means that are appropriate to the research performed.
   - While NeurIPS does not require releasing code, the conference does require all submissions to provide some reasonable avenue for reproducibility, which may depend on the nature of the contribution. For example
     (a) If the contribution is primarily a new algorithm, the paper should make it clear how to reproduce that algorithm.
     (b) If the contribution is primarily a new model architecture, the paper should describe the architecture clearly and fully.
     (c) If the contribution is a new model (e.g., a large language model), then there should either be a way to access this model for reproducing the results or a way to reproduce the model (e.g., with an open-source dataset or instructions for how to construct the dataset).
     (d) We recognize that reproducibility may be tricky in some cases, in which case authors are welcome to describe the particular way they provide for reproducibility. In the case of closed-source models, it may be that access to the model is limited in some way (e.g., to registered users), but it should be possible for other researchers to have some path to reproducing or verifying the results.

5. **Open access to data and code**

Question: Does the paper provide open access to the data and code, with sufficient instructions to faithfully reproduce the main experimental results, as described in supplemental material?

Answer: [No]

Justification: The code will be released upon acceptance. We believe that the results are easy to reproduce with the details of hypernetwork provided in Appendix B.

Guidelines:

- The answer NA means that paper does not include experiments requiring code.
- Please see the NeurIPS code and data submission guidelines (`https://nips.cc/public/guides/CodeSubmissionPolicy`) for more details.
- While we encourage the release of code and data, we understand that this might not be possible, so "No" is an acceptable answer. Papers cannot be rejected simply for not including code, unless this is central to the contribution (e.g., for a new open-source benchmark).
- The instructions should contain the exact command and environment needed to run to reproduce the results. See the NeurIPS code and data submission guidelines (`https://nips.cc/public/guides/CodeSubmissionPolicy`) for more details.
- The authors should provide instructions on data access and preparation, including how to access the raw data, preprocessed data, intermediate data, and generated data, etc.
- The authors should provide scripts to reproduce all experimental results for the new proposed method and baselines. If only a subset of experiments are reproducible, they should state which ones are omitted from the script and why.
- At submission time, to preserve anonymity, the authors should release anonymized versions (if applicable).
- Providing as much information as possible in supplemental material (appended to the paper) is recommended, but including URLs to data and code is permitted.

6. **Experimental setting/details**

Question: Does the paper specify all the training and test details (e.g., data splits, hyperparameters, how they were chosen, type of optimizer, etc.) necessary to understand the results?

Answer: [Yes]

Justification: We provide all the details of experimental setup for model training and testing in Section 4.1 and Appendix C.

Guidelines:

- The answer NA means that the paper does not include experiments.
- The experimental setting should be presented in the core of the paper to a level of detail that is necessary to appreciate the results and make sense of them.
- The full details can be provided either with the code, in appendix, or as supplemental material.

7. **Experiment statistical significance**

Question: Does the paper report error bars suitably and correctly defined or other appropriate information about the statistical significance of the experiments?

Answer: [No]

Justification: The experiments conducted in our paper do not involve the use of error bars or statistical significance analysis.

Guidelines:

- The answer NA means that the paper does not include experiments.
- The authors should answer "Yes" if the results are accompanied by error bars, confidence intervals, or statistical significance tests, at least for the experiments that support the main claims of the paper.

- The factors of variability that the error bars are capturing should be clearly stated (for example, train/test split, initialization, random drawing of some parameter, or overall run with given experimental conditions).
- The method for calculating the error bars should be explained (closed form formula, call to a library function, bootstrap, etc.)
- The assumptions made should be given (e.g., Normally distributed errors).
- It should be clear whether the error bar is the standard deviation or the standard error of the mean.
- It is OK to report 1-sigma error bars, but one should state it. The authors should preferably report a 2-sigma error bar than state that they have a 96% CI, if the hypothesis of Normality of errors is not verified.
- For asymmetric distributions, the authors should be careful not to show in tables or figures symmetric error bars that would yield results that are out of range (e.g. negative error rates).
- If error bars are reported in tables or plots, The authors should explain in the text how they were calculated and reference the corresponding figures or tables in the text.

8. **Experiments compute resources**

   Question: For each experiment, does the paper provide sufficient information on the computer resources (type of compute workers, memory, time of execution) needed to reproduce the experiments?

   Answer: [Yes]

   Justification: We provide the detailed utilization of the GPU resources, training batch size and iterations in Appendix C.

   Guidelines:

   - The answer NA means that the paper does not include experiments.
   - The paper should indicate the type of compute workers CPU or GPU, internal cluster, or cloud provider, including relevant memory and storage.
   - The paper should provide the amount of compute required for each of the individual experimental runs as well as estimate the total compute.
   - The paper should disclose whether the full research project required more compute than the experiments reported in the paper (e.g., preliminary or failed experiments that didn't make it into the paper).

9. **Code of ethics**

   Question: Does the research conducted in the paper conform, in every respect, with the NeurIPS Code of Ethics `https://neurips.cc/public/EthicsGuidelines`?

   Answer: [Yes]

   Justification: Our research conducted in the paper conforms with the NeurIPS Code of Ethics.

   Guidelines:

   - The answer NA means that the authors have not reviewed the NeurIPS Code of Ethics.
   - If the authors answer No, they should explain the special circumstances that require a deviation from the Code of Ethics.
   - The authors should make sure to preserve anonymity (e.g., if there is a special consideration due to laws or regulations in their jurisdiction).

10. **Broader impacts**

    Question: Does the paper discuss both potential positive societal impacts and negative societal impacts of the work performed?

    Answer: [NA]

    Justification: We do not believe that enhancing and accelerating diffusion models will inherently result in direct negative social impact, nor do we anticipate any significant social consequences from this optimization.

Guidelines:

- The answer NA means that there is no societal impact of the work performed.
- If the authors answer NA or No, they should explain why their work has no societal impact or why the paper does not address societal impact.
- Examples of negative societal impacts include potential malicious or unintended uses (e.g., disinformation, generating fake profiles, surveillance), fairness considerations (e.g., deployment of technologies that could make decisions that unfairly impact specific groups), privacy considerations, and security considerations.
- The conference expects that many papers will be foundational research and not tied to particular applications, let alone deployments. However, if there is a direct path to any negative applications, the authors should point it out. For example, it is legitimate to point out that an improvement in the quality of generative models could be used to generate deepfakes for disinformation. On the other hand, it is not needed to point out that a generic algorithm for optimizing neural networks could enable people to train models that generate Deepfakes faster.
- The authors should consider possible harms that could arise when the technology is being used as intended and functioning correctly, harms that could arise when the technology is being used as intended but gives incorrect results, and harms following from (intentional or unintentional) misuse of the technology.
- If there are negative societal impacts, the authors could also discuss possible mitigation strategies (e.g., gated release of models, providing defenses in addition to attacks, mechanisms for monitoring misuse, mechanisms to monitor how a system learns from feedback over time, improving the efficiency and accessibility of ML).

11. **Safeguards**

    Question: Does the paper describe safeguards that have been put in place for responsible release of data or models that have a high risk for misuse (e.g., pretrained language models, image generators, or scraped datasets)?

    Answer: [NA]

    Justification: Our paper poses no such risks.

    Guidelines:

    - The answer NA means that the paper poses no such risks.
    - Released models that have a high risk for misuse or dual-use should be released with necessary safeguards to allow for controlled use of the model, for example by requiring that users adhere to usage guidelines or restrictions to access the model or implementing safety filters.
    - Datasets that have been scraped from the Internet could pose safety risks. The authors should describe how they avoided releasing unsafe images.
    - We recognize that providing effective safeguards is challenging, and many papers do not require this, but we encourage authors to take this into account and make a best faith effort.

12. **Licenses for existing assets**

    Question: Are the creators or original owners of assets (e.g., code, data, models), used in the paper, properly credited and are the license and terms of use explicitly mentioned and properly respected?

    Answer: [Yes]

    Justification: The creators or original owners of assets used in the paper, are properly credited. Additionally, the license and terms of use associated with these assets are explicitly mentioned.

    Guidelines:

    - The answer NA means that the paper does not use existing assets.
    - The authors should cite the original paper that produced the code package or dataset.
    - The authors should state which version of the asset is used and, if possible, include a URL.

- The name of the license (e.g., CC-BY 4.0) should be included for each asset.
- For scraped data from a particular source (e.g., website), the copyright and terms of service of that source should be provided.
- If assets are released, the license, copyright information, and terms of use in the package should be provided. For popular datasets, `paperswithcode.com/datasets` has curated licenses for some datasets. Their licensing guide can help determine the license of a dataset.
- For existing datasets that are re-packaged, both the original license and the license of the derived asset (if it has changed) should be provided.
- If this information is not available online, the authors are encouraged to reach out to the asset's creators.

13. **New assets**

    Question: Are new assets introduced in the paper well documented and is the documentation provided alongside the assets?

    Answer: [NA] .

    Justification: Our paper does not release new assets.

    Guidelines:

    - The answer NA means that the paper does not release new assets.
    - Researchers should communicate the details of the dataset/code/model as part of their submissions via structured templates. This includes details about training, license, limitations, etc.
    - The paper should discuss whether and how consent was obtained from people whose asset is used.
    - At submission time, remember to anonymize your assets (if applicable). You can either create an anonymized URL or include an anonymized zip file.

14. **Crowdsourcing and research with human subjects**

    Question: For crowdsourcing experiments and research with human subjects, does the paper include the full text of instructions given to participants and screenshots, if applicable, as well as details about compensation (if any)?

    Answer: [NA] .

    Justification: Our paper does not involve crowdsourcing nor research with human subjects.

    Guidelines:

    - The answer NA means that the paper does not involve crowdsourcing nor research with human subjects.
    - Including this information in the supplemental material is fine, but if the main contribution of the paper involves human subjects, then as much detail as possible should be included in the main paper.
    - According to the NeurIPS Code of Ethics, workers involved in data collection, curation, or other labor should be paid at least the minimum wage in the country of the data collector.

15. **Institutional review board (IRB) approvals or equivalent for research with human subjects**

    Question: Does the paper describe potential risks incurred by study participants, whether such risks were disclosed to the subjects, and whether Institutional Review Board (IRB) approvals (or an equivalent approval/review based on the requirements of your country or institution) were obtained?

    Answer: [NA] .

    Justification: Our paper does not involve crowdsourcing nor research with human subjects.

    Guidelines:

    - The answer NA means that the paper does not involve crowdsourcing nor research with human subjects.

- Depending on the country in which research is conducted, IRB approval (or equivalent) may be required for any human subjects research. If you obtained IRB approval, you should clearly state this in the paper.
- We recognize that the procedures for this may vary significantly between institutions and locations, and we expect authors to adhere to the NeurIPS Code of Ethics and the guidelines for their institution.
- For initial submissions, do not include any information that would break anonymity (if applicable), such as the institution conducting the review.

16. **Declaration of LLM usage**

    Question: Does the paper describe the usage of LLMs if it is an important, original, or non-standard component of the core methods in this research? Note that if the LLM is used only for writing, editing, or formatting purposes and does not impact the core methodology, scientific rigorousness, or originality of the research, declaration is not required.

    Answer: [NA]

    Justification: The core method development in this research does not involve LLMs as any important, original, or non-standard components

    Guidelines:

    - The answer NA means that the core method development in this research does not involve LLMs as any important, original, or non-standard components.
    - Please refer to our LLM policy (`https://neurips.cc/Conferences/2025/LLM`) for what should or should not be described.